Green Chemistry

COMMUNICATION

View Article Online
View Journal | View Issue

Cite this: *Green Chem.*, 2014, **16**, 4506

Received 17th June 2014,
Accepted 22nd July 2014

DOI: 10.1039/c4gc01139b

www.rsc.org/greenchem

Hydrothermal saline promoted grafting: a route to sulfonic acid SBA-15 silica with ultra-high acid site loading for biodiesel synthesis†

C. Pirez,*‡[a] A. F. Lee,[b] J. C. Manayil,[b] C. M. A. Parlett[b] and K. Wilson*[b]

A simple grafting protocol is reported which affords a ten-fold enhancement in acid site density of mesoporous sulfonic acid silicas compared to conventional syntheses, offering improved process efficiency and new opportunities for tailored supported solid acids in sustainable chemistry.

Heterogeneous catalysis will play a critical role in the efficient conversion of biomass to fuels and chemicals, with new acid catalysts required for a range of transformations spanning dehydration, etherification, esterification and transesterification processes. The microporous nature of zeolites makes them unsuitable for such transformations with poor mass transport limiting their performance.[1] There is thus an urgent need for tailored solid acids with well-defined mesopore architectures and high surface acid site loadings for biomass utilisation.[2]

One such process whose commercial viability depends on the availability of efficient and robust solid acid catalysts is commercial biodiesel production from the transesterification and esterification of plant, algae or waste oil triglycerides (TAG) and fatty acids (FFA).[3] Biodiesel production from high FFA containing waste oils cannot be produced directly using base catalysts, and requires an acid catalysed pre-esterification step to remove FFA as FAME, prior to base catalysed TAG transesterification. The energy intensive fuel purification *via* aqueous quench step associated with these processes is detrimental to the economic viability of biodiesel production. Thus, the availability of efficient solid acid catalysts capable of simultaneous TAG and FFA conversion in waste oils would greatly improve biodiesel process efficiency[4–7] by eliminating the waste water generated from these quench steps and also offering possibilities for continuous rather than batch processes; both core principles of green chemistry.[8]

Numerous solid acid materials have been investigated for biodiesel synthesis spanning ion-exchange resins, sulphated and tungstated zirconia, ion-exchanged heteropolyacids, zeolites and sulfonic acid silicas.[5] Practical application of such solid acid catalysts is however limited by poor acid site accessibility to bulky FFA and TAG molecules and low acid site loadings; necessitating use of high catalyst quantities often >20 wt% for resins.[9] Sulfonic acid functionalised mesoporous and hierarchical meso–macroporous templated silicas are attractive solid acids designed to improve diffusion of bulky TAG and FFA molecules and active site accessibility in acid catalysed biodiesel synthesis.[10–12] While existing materials offer superior TOFs to Amberlyst-15,[12,13] low acid site loadings of ~0.4–0.7 mmol g^{-1} limit the ultimate process yields. Furthermore, use of one-pot co-condensation routes to achieve higher sulfonic acid loadings approaching the 5 mmol g^{-1} of Amberlyst lead to loss of mesoscopic order of the pore architecture.[14] Thus a post-grafting method to increase sulphonic acid loadings while retaining pore order would offer greater versatility to prepare nano-porous solid acid catalysts for biomass transformation.

The concentration of active Si–OH, particularly on calcined silicas, limits the grafting efficiency of mercaptopropyl silane (MPTMS) precursor used to form sulfonic acid groups on silica surfaces. However, as silica surfaces are sensitive to hydrothermal treatment, it was rationalised that mild hydrothermal treatment could be used to activate the surface of calcined SBA-15 and increase its capacity for grafting. NaCl is used to moderate the wall thickness and the degree of polymerization during post-synthesis hydrothermal treatments of SBA-15,[15] and also aid the dissolution of silica,[16] thus we hypothesised that addition of NaCl under mild hydrothermal conditions could promote the activation of SBA-15 surfaces for grafting. Here we report on a new hydrothermal saline promoted grafting (HSPG) method, in which the effect of [H_2O]–[NaCl] ratio

[a]*School of Chemistry, Cardiff University, Park Place, Cardiff, CF10 3AT, UK*
[b]*European Bioenergy Research Institute, School of Engineering and Applied Sciences, Aston University, Birmingham, B4 7ET, UK. E-mail: k.wilson@aston.ac.uk*

†Electronic supplementary information (ESI) available: Porosimetry data, XRD, XPS, MAS-NMR, TGA, DRIFT spectra and FFA esterification reaction profiles. See DOI: 10.1039/c4gc01139b

‡Present address: UCCS, University of Lille I, 59655 Villeneuve d'Ascq, France.

during MPTMS grafting on SBA-15 on acid site loading and associated catalyst performance is investigated.

The impact of [NaCl] on sulfonic acid loading was first investigated by porosimetry, XRD, XPS and NH_3 pulse titration (Table S1†). Acid site loading and sulfur density varies in a linear fashion with acid site density (Fig. S3†), suggesting the organosilane is uniformly dispersed with minimal agglomeration in all samples. Porosimetry and low angle XRD (Fig. S1†) evidenced that all materials retain their mesoporous structure upon sulfonic acid functionalization, with pore spacing ~10 nm. BJH analysis reveals grafting from H_2O–NaCl produces a bimodal pore size distribution with maxima ~3.6 and 4.6 nm. The relative intensity of these two components passed through a maximum for [NaCl] = 3.4 mmol $g^{-1}_{(SiO2)}$ for $PrSO_3H$/SBA-15-200, corresponding to a molar NaCl–hydroxyl ~1 and maximum incorporation of sulfonic acid groups as shown in Fig. 1. TEM (inset) shows the hexagonal pore structure of SBA-15 is retained following grafting in H_2O–NaCl, which coupled with the observed constant pore spacing from XRD, suggests the decrease in BJH pore diameter of ~1 nm upon grafting is consistent with the formation of a compact monolayer of $PrSO_3H$ groups as illustrated in Fig. 1.

Insight into the nature of the grafted sulfonic acid species formed upon grafting in H_2O–NaCl as compared to conventional toluene grafting or one-pot methods was further studied by MAS-NMR, TGA and XPS. The absence of any disulphide species peaks at 41 and 23 ppm by ^{13}C MAS-NMR,[17] $-S^{(II)}$ peak at 162 eV in S 2p XPS[14] and weight loss <350 °C in TGA[18] (Fig. S3–6†) confirmed the total oxidation of grafted MPTS to sulfonic acid groups. ^1H MAS-NMR (Fig. S7†) revealed δ ^1H of the hydrated surface $SO_2OH_x(H_2O)$ group shifts over the range 5–7 ppm as a function of loading. This feature is associated with protons from H_2O bound to hydrated sulfonic acid groups,[19–21] with fast proton exchange between water and the sulfonic acid group leading to a single peak.[21,22] The striking correlation between δ ^1H and acid site density is thus indicative of increased acid strength,[19] indicating enhanced cooperative effects,[23,24] increasing the surface acid site density from 0.7 to 2.2 mmol (H^+) g^{-1}. Furthermore NH_3 TPD peak maxima shown in Fig. S8† increase from Tol-$PrSO_3H$/SBA-15 < $PrSO_3H$-SBA-15-OP < $PrSO_3H$/SBA-15-200, confirming enhanced acid strength.

^{29}Si CP-MAS NMR (Fig. S9†) was employed to quantify the relative concentrations of Qn and Tm modes of the grafted organosilane[18,22,25] and thus explore the mode of attachment (Table S2†). A slight decrease in the Q3 species was observed upon grafting in toluene indicative of attachment at isolated hydroxyl sites, while the intense Q3 band for the $PrSO_3H$-SBA-15-OP is consistent with an uncalcined material with less cross-linking and Si–O–Si bridges. In contrast the Q2 species of HSPG samples decreased strongly, consistent with preferential grafting at geminal silanols. The increased grafting efficiency under HSPG conditions is thus attributed to partial 'dissolution' of the SBA-15 surface activating Si–O–Si groups towards grafting. Enhanced surface cross-linking following HSPG is also evident from the increase in Tm coordinated species which would lead to a more stable coating. Changes in the Si–OH region observed by DRIFTS (Fig. S10 and Scheme 1a†) further support these observations, with HSPG showing a complete loss of isolated, germinal and vicinal modes and thus reaction of these groups with the silane. A possible mechanism for the role of NaCl in promoting surface grafting is outlined in Scheme S1b† which illustrates how hydrothermal treatment in H_2O–NaCl could open Si–O–Si bridges, with the resulting Si–OH stabilised by ionic interactions with Cl^- prior to grafting of MPTS, akin to the way that ionic liquids are proposed to weaken hydrogen bonding in cellulose.[26] The decreased grafting efficiency above a 1 : 1 ratio of NaCl–OH presumably reflects reduced silanol accessibility from excess surface adsorbed salt. The physical properties of HSPG and conventional sulfonic acid silicas are compared in Table S3 and Fig. S11–12,† with HRTEM and XRD measurements showing the hexagonal pore structure is maintained.

The optimum HSPG prepared catalyst $PrSO_3H$/SBA-15-200 was subsequently evaluated in FFA esterification and TAG transesterification and compared to conventional grafted or one-pot materials. The conversion of tributyrin and tripalmitin during transesterification was observed to follow the order $PrSO_3H$/SBA-15-200 > $PrSO_3H$/SBA-15-OP > $PrSO_3H$/SBA-15-Tol, with $PrSO_3H$/SBA-15-200 increasing the FAME yield from tripalmitin by a factor of three over conventional grafted materials (Fig. 2). Despite having an inferior pore diameter, the corresponding turnover number (TON) for $PrSO_3H$/SBA-15-200 in transesterification exceeds conventional materials (Table S4†). Transesterification is rate-limited by protonation of the ester[27] and thus sensitive to catalyst acid strength, hence enhanced performance can be attributed to

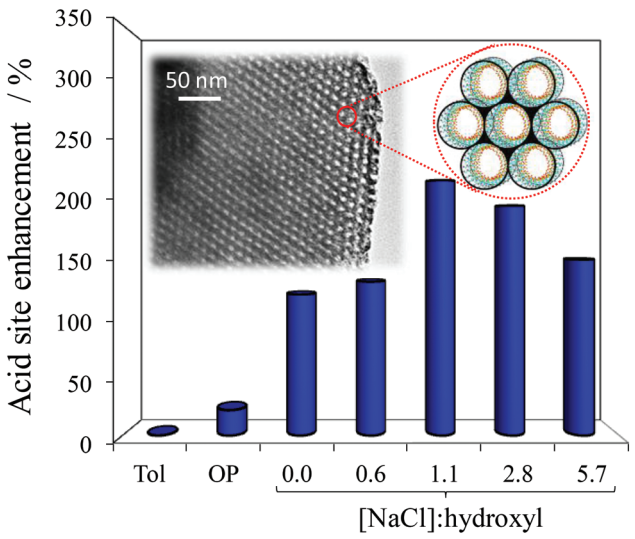

Fig. 1 Effect of [NaCl]–hydroxyl ratio during –$PrSO_3H$ grafting in H_2O–NaCl on resulting acid site loading, as compared to conventional toluene grafted and one-pot co-condensed materials. Inset shows HRTEM for [NaCl]–hydroxyl = 1.1, confirming ordered mesoporosity is retained. (Hydroxyl density for parent SBA-15 calculated to be 3 mmol g^{-1} from TGA over the range 200–1000 °C.)

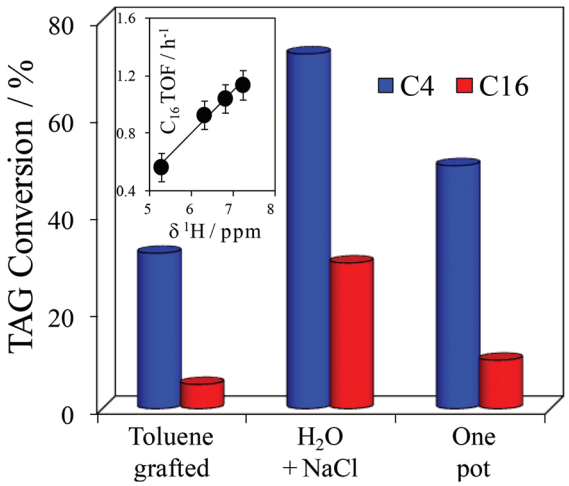

Fig. 2 Conversion of glyceryl tributyrate and tripalmitate with methanol at 80 °C respectively after 24 hours reaction over PrSO3H/SBA-15-Tol, $PrSO_3H$/SBA-15-200 and $PrSO_3H$-SBA-15-OP. Inset shows the correlation between TOF for tripalmitin transesterification with δ ^{1}H.

the increased cooperative effect and strength of sulfonic acid groups in $PrSO_3H$/SBA-15-200, as earlier indicated by NH_3 TPD and δ ^{1}H in NMR. Indeed the inset to Fig. 2 shows a strong correlation between TOF for tripalmitin transesterification and δ ^{1}H shift. Fig. S13† shows that $PrSO_3H$/SBA-15-200 also out performs both one-pot sulfonic acids and Amberlyst-15 in palmitic acid esterification, while showing a two-fold increase in reaction rate compared to grafted catalysts. Palmitic acid conversions of 97% observed after 24 h are particularly impressive given only 2 wt% $PrSO_3H$/SBA-15-200 was employed: for comparable conditions in the literature, acid resin loadings >20 wt% are typically reported as required to achieve 85% conversion of FFA in waste oil.[9]

In summary, HSPG offers a new route to produce high loaded sulfonic acid silicas, increasing the acid site loading five-fold over conventional methods. Enhanced acidic properties lead to a versatile catalyst with superior performance in TAG and FFA transformations. Future work will investigate the use of HSPG on interconnected and larger pore template silicas such as KIT-6 and hierarchical macro–mesoporous supports, shown to reduce diffusion limitations in esterification and transesterification reactions,[10–12] improving the potential for commercial implementation of more complex preformed architectures. The use of such materials in intensive reactors such as oscillatory baffled continuous flow reactors[28] will also be explored. In addition these methods could prove valuable for derivatisation of magnetically separable nanoparticulate catalysts with high sulfonic acid loadings.[29,30]

Acknowledgements

We thank the EPSRC (EP/K000616/2, EP/K000616/2 and EP/G007594/4) for financial support and a Leadership Fellowship (AFL), and the Royal Society for the award of an Industry Fellowship (KW). We also acknowledge the kind assistance of Mark Isaacs for XPS analysis and D.C. Apperley at the EPSRC UK National Solid-state NMR Service at Durham.

Notes and references

1 J. H. Clark, *Acc. Chem. Res.*, 2002, **35**, 791–797.
2 R. Rinaldi and F. Schuth, *Energy Environ. Sci.*, 2009, **2**, 610–626.
3 R. Luque, J. C. Lovett, B. Datta, J. Clancy, J. M. Campelo and A. A. Romero, *Energy Environ. Sci.*, 2010, **3**, 1706–1721.
4 J. M. Marchetti, V. U. Miguel and A. F. Errazu, *Fuel Process. Technol.*, 2008, **89**, 740–748.
5 J. A. Melero, J. Iglesias and G. Morales, *Green Chem.*, 2009, **11**, 1285–1308.
6 E. Lotero, Y. Liu, D. E. Lopez, K. Suwannakarn, D. A. Bruce and J. G. Goodwin, *Ind. Eng. Chem. Res.*, 2005, **44**, 5353–5363.
7 Y. Feng, A. Zhang, J. Li and B. He, *Bioresour. Technol.*, 2011, **102**, 3607–3609.
8 P. T. Anastas, L. B. Bartlett, M. M. Kirchhoff and T. C. Williamson, *Catal. Today*, 2000, **55**, 11–22.
9 Y. Feng, B. He, Y. Cao, J. Li, M. Liu, F. Yan and X. Liang, *Bioresour. Technol.*, 2010, **101**, 1518–1521.
10 J. Dhainaut, J.-P. Dacquin, A. F. Lee and K. Wilson, *Green Chem.*, 2010, **12**, 296–303.
11 J. P. Dacquin, A. F. Lee, C. Pirez and K. Wilson, *Chem. Commun.*, 2012, **48**, 212–214.
12 C. Pirez, J.-M. Caderon, J.-P. Dacquin, A. F. Lee and K. Wilson, *ACS Catal.*, 2012, **2**, 1607–1614.
13 J. A. Melero, L. F. Bautista, G. Morales, J. Iglesias and R. Sánchez-Vázquez, *Chem. Eng. J.*, 2010, **161**, 323–331.
14 K. Wilson, A. F. Lee, D. J. Macquarrie and J. H. Clark, *Appl. Catal., A*, 2002, **228**, 127–133.
15 F. Zhang, Yan, H. Yang, Meng, Y. Y. Meng, C. Yu, B. Tu and D. Zhao, *J. Phys. Chem. B*, 2005, **109**, 8723–8732.
16 J. P. Icenhower and P. M. Dove, *Geochim. Cosmochim. Acta*, 2000, **64**, 4193–4203.
17 W. M. Van Rhijn, D. E. De Vos, B. F. Sels and W. D. Bossaert, *Chem. Commun.*, 1998, 317–318.
18 S.-Y. Chen, T. Yokoi, C.-Y. Tang, L.-Y. Jang, T. Tatsumi, J. C. C. Chan and S. Cheng, *Green Chem.*, 2011, **13**, 2920–2930.
19 G. Ye, N. Janzen and G. R. Goward, *Macromolecules*, 2006, **39**, 3283–3290.
20 G. Morales, G. Athens, B. F. Chmelka, R. van Grieken and J. A. Melero, *J. Catal.*, 2008, **254**, 205–217.
21 A. Simperler, R. G. Bell and M. W. Anderson, *J. Phys. Chem. B*, 2004, **108**, 7142–7151.
22 R. Kanthasamy, I. K. Mbaraka, B. H. Shanks and S. C. Larsen, *Appl. Magn. Reson.*, 2007, **32**, 513–526.
23 I. K. Mbaraka and B. H. Shanks, *J. Catal.*, 2006, **244**, 78–85.
24 J.-P. Dacquin, H. E. Cross, D. R. Brown, T. Duren, J. J. Williams, A. F. Lee and K. Wilson, *Green Chem.*, 2010, **12**, 1383–1391.

25 H.-H. G. Tsai, P.-J. Chiu, G.-L. Jheng, C.-C. Ting, Y.-C. Pan and H.-M. Kao, *J. Colloid Interface Sci.*, 2011, **359**, 86–94.
26 R. C. Remsing, R. P. Swatloski, R. D. Rogers and G. Moyna, *Chem. Commun.*, 2006, 1271–1273.
27 D. E. López, J. G. Goodwin Jr. and D. A. Bruce, *J. Catal.*, 2007, **245**, 381–391.
28 V. C. Eze, A. N. Phan, C. Pirez, A. P. Harvey, A. F. Lee and K. Wilson, *Catal. Sci. Technol.*, 2013, **3**, 2373–2379.
29 M. B. Gawande, P. S. Branco and R. S. Varma, *Chem. Soc. Rev.*, 2013, **42**, 3371–3393.
30 M. B. Gawande, A. K. Rathi, I. D. Nogueira, R. S. Varma and P. S. Branco, *Green Chem.*, 2013, **15**, 1895–1899.